NANO LETTERS

pubs.acs.org/NanoLett

Catalyst-Free InGaN/GaN Nanowire Light Emitting Diodes Grown on (001) Silicon by Molecular Beam Epitaxy

Wei Guo, Meng Zhang, Animesh Banerjee, and Pallab Bhattacharya*

Center for Nanoscale Photonics and Spintronics, University of Michigan, Ann Arbor, Michigan 48109-2122

ABSTRACT Catalyst-free growth of (In)GaN nanowires on (001) silicon substrate by plasma-assisted molecular beam epitaxy is demonstrated. The nanowires with diameter ranging from 10 to 50 nm have a density of $1-2 \times 10^{11}$ cm^{-2}. P- and n-type doping of the nanowires is achieved with Mg and Si dopant species, respectively. Structural characterization by high-resolution transmission electron microscopy (HRTEM) indicates that the nanowires are relatively defect-free. The peak emission wavelength of InGaN nanowires can be tuned from ultraviolet to red by varying the In composition in the alloy and "white" emission is obtained in nanowires where the In composition is varied continuously during growth. The internal quantum efficiency varies from 20−35%. Radiative and nonradiative lifetimes of 5.4 and 1.4 ns, respectively, are obtained from time-resolved photoluminescence measurements at room temperature for InGaN nanowires emitting at $\lambda = 490$ nm. Green- and white-emitting planar LEDs have been fabricated and characterized. The electroluminescence from these devices exhibits negligible quantum confined Stark effect or band-tail filling effect.

KEYWORDS InGaN nanowire, carrier lifetime, nanowire LEDs, graded composition nanowires

Progress in solid state lighting at the present time primarily involves research and development of visible nitride-based light emitting diodes (LEDs) and perhaps lasers in the future.[1,2] However, this development has been impeded due to a variety of reasons: the lack of high-quality and low-cost GaN substrates, necessitating epitaxy on substrates with large lattice mismatch; poor efficiency of green-emitting LEDs, termed the "green gap";[3,4] and the catastrophic drop in efficiency at high injection currents, termed the "efficiency droop".[5] The last two deleterious effects are directly or indirectly related to the high density of dislocations caused by lattice-mismatched epitaxy. In addition, currently used "white" devices include phosphor-coated LEDs,[6] dichromatic blue/green LEDs,[7] CdSe/ZnS nanocrystals for conversion into red light,[8] prestrained growth of InGaN wells,[9] structure-controlled GaN microfacets,[10] and so forth. However, the light generated from these devices is generally bluish with poor color chromaticity and low efficiency. Successful growth of GaN and InGaN nanowires on silicon and other mismatched substrates has been demonstrated recently.[11−14] The nanowires exhibit significantly reduced defect density due to their large surface-to-volume ratio. A reduced strain distribution in the nanostructures also leads to a weaker piezoelectric polarization field. Other advantages include large light extraction efficiency and the compatibility with low-cost, large area silicon substrates. Most of the work reported on III−N nanowires has focused on materials studies and optically pumped devices.[15] Reports have also been made of electrically injected single nanowire LEDs on foreign substrates and LEDs with nanowire ensembles grown on (111) Si substrates.[16−18] However, a single nanowire device involves complicated nanowire transfer and low yield and (111) Si is not quite compatible with complementary metal oxide semiconductor (CMOS) technology.

In the study reported here, we have conducted a detailed investigation of the molecular beam epitaxial (MBE) growth of (In)GaN nanowires directly on (001) Si in the absence of a foreign metal catalyst. The structural and optical characteristics of the nanowires have been measured and are discussed. P- and n-type doping of the nanowires is accomplished with Mg and Si, respectively. Finally, LEDs have been fabricated with an ensemble of nanowires and the characteristics of these devices are also presented.

GaN and (In)GaN nanowires were grown on (001) Si substrates in a Veeco plasma-assisted molecular beam epitaxy (PA-MBE) system. The native oxide was removed from the substrate surface before epitaxy by the standard technique, which involves a rinse in HF-H_2O solution and heat treatment in the growth chamber at 900 °C for 30 min under a vacuum of 1×10^{-9} Torr. The substrate temperature was lowered to 800 °C and a few monolayers of Ga were deposited with a Ga flux of 1.5×10^{-7} Torr in the absence of N. GaN nanowires were then grown at 800 °C at a rate of 300 nm/h under N-rich conditions. The Ga flux was maintained at 1.5×10^{-7} Torr and the N flow rate was held constant at 1 sccm. To grow (In)GaN nanowires, 300 nm of a seed GaN nanowire was first grown under the conditions outlined above. The growth temperature was then lowered to 550 °C. The Ga flux was held constant at 1×10^{-7} Torr

* To whom correspondence should be addressed. E-mail: pkb@eecs.umich.edu. Phone: 734-763-6678. Fax: 734-763-9324.

Received for review: 03/23/2010
Published on Web: 08/11/2010

DOI: 10.1021/nl101027x | *Nano Lett.* **2010,** *10,* 3355–3359

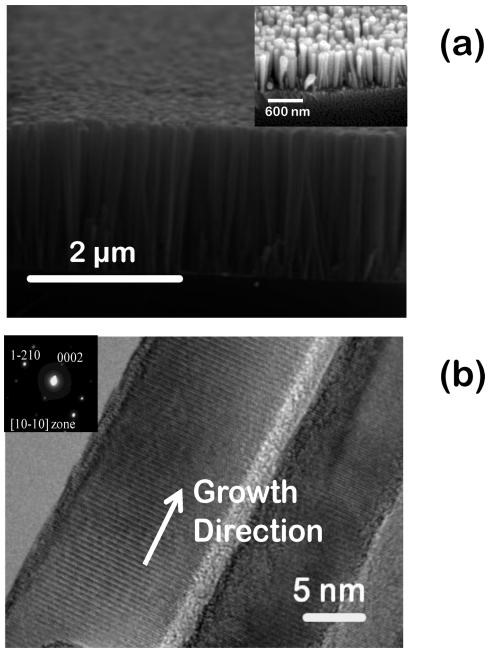

FIGURE 1. (a) Cross-sectional SEM image of catalyst-free InGaN NWs grown by plasma-assisted MBE on (001) Si. The vertically aligned InGaN nanowires are 10 −50 nm in diameter and 2 μm long. The density of the nanowires varies in the range of $1-2 \times 10^{11}$ cm^{-2} under the growth conditions described in the text; the inset oblique view SEM image of n-GaN/InGaN/p-GaN nanowires shows that the nanowires are vertically aligned and separated at the top. (b) HRTEM image of InGaN nanowire of 20 nm diameter. The inset shows the selective area diffraction pattern. Defects are generally not observed.

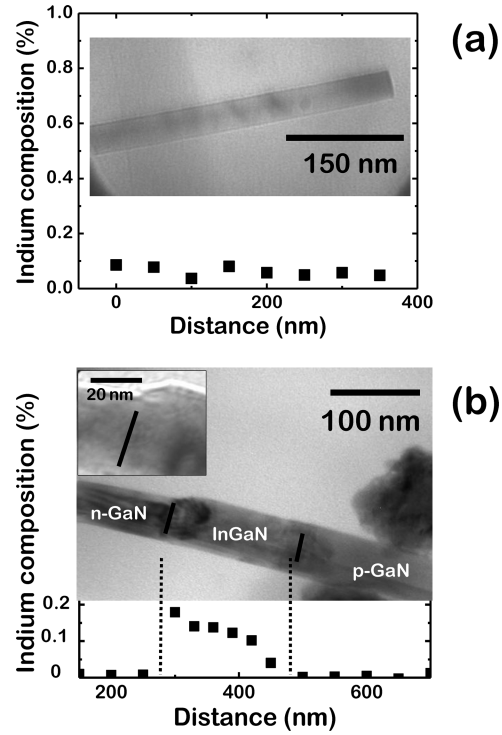

FIGURE 2. (a) The indium composition distribution along a InGaN nanowire obtained from energy dispersive X-ray (EDX) measurement. A small variation of indium composition along the length of the nanowire is observed. The inset shows a low magnification TEM image of a single InGaN nanowire which illustrates that the nanowire has uniform diameter and no observable defects are present. (b) A TEM image of a n-GaN/InGaN/p-GaN p-i-n nanowire heterostructure and the indium composition along the entire length, as measured by EDX. The indium composition was continuously varied in the InGaN section during epitaxy, which is confirmed by the data. Also noticeable is the fact that the diameter of the nanowire increases slightly in going from GaN to InGaN at the n-GaN/InGaN heterointerface. This is probably a consequence of the lower growth temperature of InGaN compared to that of GaN. The inset shows a higher magnification TEM image of the n-GaN/InGaN interface, where no defects are observed.

and the In flux was varied from 3.5×10^{-8} to 2.5×10^{-7} Torr to grow (In)GaN nanowires with different In compositions. In some samples, the In composition was continuously varied along the length of the nanowires to provide a broad luminescence spectrum. To study a single nanowire by transmission electron microscopy (TEM), the nanowires were stripped off from the substrate into an ethanol solution and subsequently dried on a carbon-coated copper grid.

A cross-sectional scanning electron microscope (SEM) image of an InGaN nanowire sample grown on (001) Si is shown in Figure 1a. It is apparent that the nanowires with an areal density $1-2 \times 10^{11}$ cm^{-2} are vertically aligned. The inset oblique view SEM image of n-GaN/InGaN/p-GaN nanowires shows that the nanowires are vertically aligned and separated at the top. The structural properties of the nanowires were investigated by high-resolution TEM (HRTEM) imaging. Figure 1b shows such an image of an InGaN nanowire indicating that it is structurally uniform with a constant diameter of ~20 nm along the length and free of dislocations. The bright line in the middle is the boundary between two nanowires, since both appear in this image. The selected area diffraction (SAD) pattern in the inset reveals that the entire wire is single crystal with wurtzite structure and the *c*-plane is normal to the growth direction. It is derived from the diffraction pattern that the lattice constant of this nanowire is 5.4 Å that corresponds to an In composition of 25%.[19] Figure 2a shows the indium distribution along a InGaN nanowire obtained from energy dispersive X-ray (EDX) measurement. A small variation of indium composition along the length of the nanowire is observed. The inset of Figure 2a shows a low-magnification TEM image of a single InGaN nanowire that illustrates that the nanowire has uniform diameter and no observable defects are present. Figure 2b shows a TEM image of a n-GaN/InGaN/p-GaN p-i-n nanowire heterostructure and the indium composition along the entire length, as measured by EDX. The indium composition was continuously varied in the InGaN section during epitaxy, which is confirmed by the data. It is worthy to notice that the EDX measurement is not calibrated and the actual indium composition may be varied from the measured data. Also noticeable is the fact that the diameter of the nanowire increases slightly in going from GaN to InGaN at the n-GaN/InGaN heterointerface. This is probably a consequence of the lower growth temperature of InGaN compared to that of

DOI: 10.1021/nl101027x | *Nano Lett.* **2010,** *10,* 3355–3359

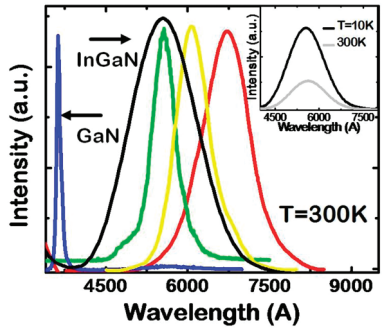

FIGURE 3. Room-temperature photoluminescence spectra of InGaN NWs with varying In content. The PL is shifted to longer wavelengths by increasing the In composition. The broad spectrum is obtained from a nanowire sample in which the In composition was continuously varied (along length) during epitaxy. The inset shows the temperature dependence of the broad luminescence with emission peak at 580 nm from a 300 nm long nanowire with continuously varying In composition.

GaN. The inset shows a higher magnification TEM image of the n-GaN/InGaN interface, where no defects are observed.

The optical properties of the nanowires were investigated by temperature-dependent photoluminescence (PL) and time-resolved PL (TRPL) measurements. Figure 3 shows room temperature PL spectra from InGaN nanowire ensembles having different In content. It is noticed that a large tunability of the output spectrum can be obtained by varying the In content in the nanowires. The emission line width (fwhm) progressively increases in going to longer wavelength emission, which is largely due to increased alloy broadening with higher In content in the nanowires. It is also important to note that no defect-related yellow band is observed in the emission spectra, which is further evidence of the good crystalline quality of the nanowires. The figure also depicts the PL spectrum obtained from a sample in which the In composition is continuously varied. The line width is 150 nm. From temperature-dependent PL measurements made with a "white" nanowire sample emitting with peak at 580 nm, as shown in the inset, an internal quantum efficiency (IQE) of 30% is derived, assuming that the IQE is 100% at 10 K. We also find that the IQE decreases from 30 to ~20% with increasing the wire length, which we believe is due to increasing strain accumulation.

Time-resolved PL measurements were made on InGaN nanowire samples as a function of the emission energy with a frequency-tripled (260 nm) mode-locked Tsunami Al_2O_3:Ti laser (pulse width 130 fs; repetition rate 80 MHz). The beam was focused to a ~10 μm^2 spot through a long working distance 20× microscopic objective. PL was analyzed by an Acton SpectraPro-2558 spectrometer (resolution 0.05 nm) and detected by a Picoquant Single Photon Avalanche Diode with a time resolution of 40 ps. The measured data are shown in Figure 4a. The decay times were fitted by a stretched exponential model $I = I_o \exp[-(t/\tau)^{\beta}]$.[20] For the peak energy (490 nm), the decay time is 1.12 ns and the stretching parameter is 0.74 (Figure 4b). Nanoscale fluctuations of In mole fraction are responsible for the nonmonoexponential decay.[21] Shown in Figure 4c are the decay times as a function of emission energy, varying from 0.31 to 1.98 ns. It may be noted that the PL decay is faster at higher photon energies. This is due to the larger radiative recombination rate in the nanowires with smaller In mole fraction (larger bandgap). Furthermore, by using equations $1/\tau = 1/\tau_r + 1/\tau_{nr}$ and $\eta_{int} = 1/(1 + \tau_r/\tau_{nr})$, the radiative ($\tau_r$) and nonradiative ($\tau_{nr}$) lifetimes for the peak emission wavelength were calculated as 5.4 and 1.4 ns, respectively. Here the IQE (η_{int}) was calculated to be 20.6% from temperature dependent PL measurements. The radiative lifetimes in InGaN NWs measured here are smaller than that measured in quantum wells,[22] possibly due to the confinement of carriers in the radial direction and weaker piezoelectric field due to reduced strain in the wires. However, the nonradiative lifetime is also small, which is attributed to surface states arising from the large surface-to-volume ratio.

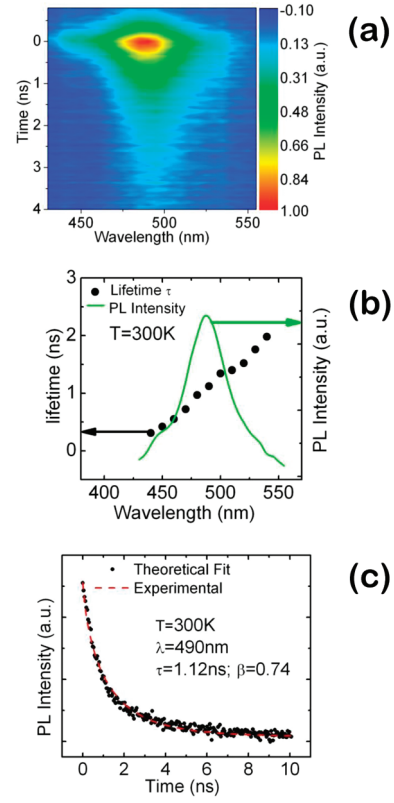

FIGURE 4. Results obtained from time-resolved photoluminescence measurements: (a) color chart depicting decay of luminescence from a nanowire with emission peak at 490 nm; (b) variation of PL peak intensity with time; and (c) variation of calculated and measured recombination lifetimes with wavelength.

Light-emitting diodes were fabricated with epitaxially grown p-i-n InGaN/GaN green- and "white"-emitting nanowires. The diode samples were grown on n-type (001) Si. Three hundred nanometers of Si-doped GaN nanowire is first grown, followed by 300 nm undoped InGaN with fixed or continuously varied In composition and 150 nm Mg-doped p-type GaN on top. The nanowires were planarized with a

DOI: 10.1021/nl101027x | *Nano Lett.* **2010,** *10,* 3355–3359

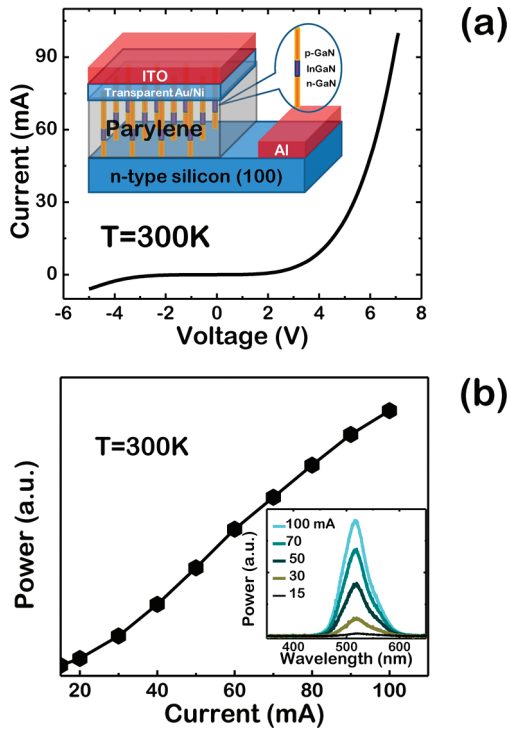

FIGURE 5. (a) Room temperature current−voltage characteristics of nanowire LEDs. The fabricated device on (001) Si is schematically shown in the inset; (b) measured electroluminescence showing variation of peak intensity with injection current. The corresponding variation in the output spectrum is shown in the inset. There is no observed shift of the emission peak with increased injection current.

parylene-insulating layer and covered with 5 nm/5 nm Ni/Au and 250 nm indium tin oxide (ITO) as the top ohmic contact to the p-GaN nanowires. Aluminum was deposited on the n-type Si to form the bottom electrode. Both parylene and ITO are nearly transparent to visible light. Figure 5 depicts the measured room temperature current−voltage ($I-V$) characteristics of a typical diode, which is schematically shown in the inset. A turn-on voltage of has been varied from 15 to 100 mA. There are several important features in the data of Figure 5b. No saturation is observed in the light−current ($L-I$) characteristics up to 100 mA (which translates to an approximate current density of 54 A/cm^2 with the mesa dimension of 600 × 600 μm and 50% filling factor of the nanowires). The measurements have been made without any heat-sinking or cooling. The emission peak is at 520 nm and the line width (fwhm) is ∼50 nm (250 meV). In particular, the emission peak does not exhibit neither red nor blue shift with increasing carrier injection, which are usually observed in InGaN/GaN quantum well (QW) or quantum dot heterostructures due to piezoelectricity-induced quantum-confined Stark effect,[23,24] or band-tail filling effect,[25−27] respectively. Since bulk InGaN nanowires form the active region of the LEDs characterized in this study, quantum confinement is very weak along the growth direction (c-axis). Thus the Stark effect is expected to be small. Band-tail filling effect due to compositional inhomogeneity and alloy disorder can be present in the nanowires,[28] but the invariant emission peak wavelength with respect to injection current suggests that such effects are negligible. It is also confirmed by narrower emission line width compared with normal epitaxial grown InGaN layers with the same indium composition.[29] Figure 6 shows the $L-I$ characteristics of the "white" LED made with compositionally graded InGaN nanowires. The electroluminescence spectrum and an image of the emitted white light are shown in the inset. The Commission Internationale de l'Eclairage (CIE) chromaticity coordinates of $x = 0.31$ and $y = 0.36$ are derived by analyzing the electroluminescence spectrum of our "white" nanowire LEDs under a forward-bias current of 300 mA. The correlated color temperatures (CCT) of 5500−6500 K are also derived from the Planckian locus.

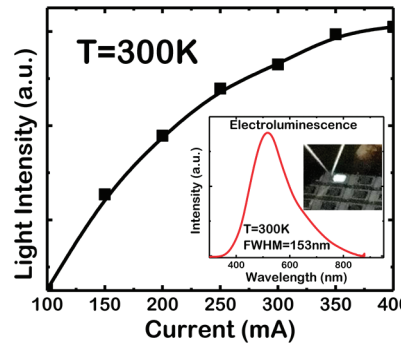

FIGURE 6. Measured light−current characteristics of "white" InGaN nanowire LED in which In composition varies along the length of nanowires. Insets show the electroluminescence spectrum and microscope image of white light emission.

In conclusion, experimental results on catalyst-free growth of InGaN nanowires are presented. The nanowires grow vertically aligned and with a high density of 1−2 × 10^{11} cm^{-2}. Structural characterization with SEM, TEM, HRTEM,and electron diffraction indicates that the nanowires crystallize in the wurtzite structure with the c-plane normal to the growth direction and are relatively defect-free. The emission of the nanowires can be tuned from UV to red by varying the In composition. InGaN nanowires with very broad (white) emission spectra can be obtained by varying the In composition continuously during epitaxy. Short radiative and nonradiative lifetime of 5.4 and 1.4 ns, respectively, at room temperature, are measured in the nanowires by TRPL measurements. P- and n-doped nanowires and p-i-n nanowire LED heterostructures were also grown and the fabricated devices were characterized. Green and white LEDs exhibit good electroluminescence characteristics and the emission peak position of green LEDs remains invariant in wavelength with increasing current injection. Further work is under way to characterize the device efficiencies. Nonetheless, the characteristics reported here indicate that nanowire LEDs after some improvement in growth and fabrication can become serious contenders in silicon photonics and solid-state lighting applications.

DOI: 10.1021/nl101027x | *Nano Lett.* **2010,** *10,* 3355–3359

Acknowledgment. This work is supported by Air Force Office of Scientific Research (AFOSR) under Grant FA9550-09-1-0634.

REFERENCES AND NOTES

(1) Schubert, E. F.; Kim, J. K. *Science* **2005**, *308*, 1274–1278.
(2) Schubert, E. F. *Light Emitting Diodes*; Cambridge University Press: New York, 2003.
(3) Nakamura, S.; Mukai, T.; Senoh, M. *J. Appl. Phys.* **1994**, *76*, 8189–8191.
(4) Akasaki, I.; Amano, H. *Jpn. J. Appl. Phys.* **1997**, *36*, 5393–5408.
(5) Mukai, T.; Yamada, M.; Nakamura, S. *Jpn. J. Appl. Phys.* **1999**, *38*, 3976–3981.
(6) Mueller-Mach, R.; Mueller, G. O.; Krames, M. R.; Trottier, T. *IEEE J. Sel. Top. Quantum Electron.* **2002**, *8*, 339–345.
(7) Lee, Y. J.; Lin, P. C.; Lu, T. C.; Kuo, H. C.; Wang, S. C. *Appl. Phys. Lett.* **2007**, *90*, 161115.
(8) Chen, H.-S.; Yeh, D.-M.; Lu, C.-F.; Huang, C.-F.; Shiao, W.-Y.; Huang, J. J.; Yang, C. C.; Liu, I. S.; Su, W.-F. *IEEE Photonics Technol. Lett.* **2006**, *18*, 1430–1432.
(9) Huang, C.-F.; Lu, C.-F.; Tang, T.-Y.; Huang, J.-J.; Yang, C. C. *Appl. Phys. Lett.* **2007**, *90*, 151122.
(10) Ueda, M.; Kondou, T.; Hayashi, K.; Funato, M.; Kawakami, Y.; Narukawa, Y.; Mukai, T. *Appl. Phys. Lett.* **2007**, *90*, 171907.
(11) Calarco, R.; Meijers, R. J.; Debnath, R. K.; Stoica, T.; Sutter, E.; Lüth, H. *Nano Lett.* **2007**, *7*, 2248–2251.
(12) Cerutti, L.; Ristic, J.; Fernandez-Garrido, S.; Calleja, E.; Trampert, A.; Ploog, K. H.; Lazic, S.; Calleja, J. M. *Appl. Phys. Lett.* **2006**, *88*, 213114.
(13) Kuykendall, T.; Ulrich, P.; Aloni, S.; Yang, P. *Nat. Mater.* **2007**, *6*, 951–956.
(14) Armitage, R.; Tsubaki, K. *Nanotechnology* **2010**, *21*, 195202.
(15) Qian, F.; Li, Y.; Gradecak, S.; Park, H.-G.; Dong, Y.; Ding, Y.; Wang, Z. L.; Lieber, C. M. *Nat. Mater.* **2008**, *7*, 701–706.
(16) Sekiguchi, H.; Kishino, K.; Kikuchi, A. *Electron. Lett.* **2008**, *44*, 151–152.
(17) Kikuchi, A.; Kawai, M.; Tada, M.; Kishino, K. *Jpn. J. Appl. Phys.* **2004**, *43*.
(18) Zhong, Z.; Qian, F.; Wang, D.; Lieber, C. M. *Nano Lett.* **2003**, *3*, 343–346.
(19) O'Donnell, K. P.; et al. *J. Physics: Condens. Matter* **2001**, *13*, 6977.
(20) Krestnikov, I. L.; Ledentsov, N. N.; Hoffmann, A.; Bimberg, D.; Sakharov, A. V.; Lundin, W. V.; Tsatsul'nikov, A. F.; Usikov, A. S.; Alferov, Z. I.; Musikhin, Y. G.; Gerthsen, D. *Phys. Rev. B* **2002**, *66*, 155310.
(21) Pophristic, M.; Long, F. H.; Tran, C.; Ferguson, I. T.; Karlicek, R. F., Jr. *Appl. Phys. Lett.* **1998**, *73*, 3550–3552.
(22) Chen, C.-Y.; Lu, Y.-C.; Yeh, D.-M.; Yang, C. C. *Appl. Phys. Lett.* **2007**, *90*, 183114.
(23) Miller, D. A. B.; Chemla, D. S.; Damen, T. C.; Gossard, A. C.; Wiegmann, W.; Wood, T. H.; Burrus, C. A. *Phys. Rev. Lett.* **1984**, *53*, 2173.
(24) Peng, L.-H.; Chuang, C.-W.; Lou, L.-H. *Appl. Phys. Lett.* **1999**, *74*, 795–797.
(25) Kuokstis, E.; Yang, J. W.; Simin, G.; Khan, M. A.; Gaska, R.; Shur, M. S. *Appl. Phys. Lett.* **2002**, *80*, 977–979.
(26) Morgan, T. N. *Phys. Rev.* **1965**, *139*, A343.
(27) Narukawa, Y.; Kawakami, Y.; Funato, M.; Fujita, S.; Fujita, S.; Nakamura, S. *Appl. Phys. Lett.* **1997**, *70*, 981–983.
(28) Eliseev, P.; Osinski, M.; Lee, J.; Sugahara, T.; Sakai, S. *J. Electron. Mater.* **2000**, *29*, 332–341.
(29) Naranjo, F. B.; Fernández, S.; Sánchez-García, M. A.; Calle, F.; Calleja, E.; Trampert, A.; Ploog, K. H. *Mater. Sci. Eng. B* **2002**, *93*, 131–134.

DOI: 10.1021/nl101027x | *Nano Lett.* **2010,** *10,* 3355–3359